



Artificial signal transduction triggered by molecular photoisomerization in lipid membranes

Kai Ye^{a,1}, Zhicheng Ye^{a,1}, Chuantao Wang^a, Zhilai Luo^a, Cheng Lian^a, Chunyan Bao^{a,b,*}

^a Shanghai Key Laboratory of Functional Materials Chemistry, School of Chemistry & Molecular Engineering, East China University of Science & Technology, Shanghai 200237, China

^b State Key Laboratory of Bioreactor Engineering, Shanghai Frontiers Science Center of Optogenetic Techniques for Cell Metabolism, School of pharmacy, East China University of Science and Technology, Shanghai 200237, China

ARTICLE INFO

Article history:

Received 22 February 2024

Revised 16 May 2024

Accepted 20 May 2024

Available online 21 May 2024

Keywords:

Artificial signal transduction

Photoisomerization

Azobenzene

ON/OFF switch

Lipid membranes

ABSTRACT

Inspired by the light-dependent signal transduction in nature, we herein report a fully synthetic receptor **AZO** with the capacity of transmembrane signaling, working by photo-induced change of molecular conformation. Our receptor has an anchoring group, a rigid and photoresponsive transmembrane unit and a pre-catalyst tailgroup. After doping in lipid membranes, **AZO** is membrane anchored and the extended *trans*-isomer enables the tailgroup to bind with intravesicular Zn^{2+} , thereby achieving enzyme activation and triggering downstream events (ester hydrolysis). However, the shortened *cis*-isomer pulls the tailgroup into lipids, thereby preventing the complexation and all transduction processes. Upon alternative irradiation of ultraviolet (UV) and visible light, the transduction process can be reversible switch between "ON" and "OFF", achieving light signal transduction. This study provides a new strategy for future design of artificial signal transduction receptors.

© 2025 Published by Elsevier B.V. on behalf of Chinese Chemical Society and Institute of Materia Medica, Chinese Academy of Medical Sciences.

The complex transmembrane receptors, embedded on the cell membrane, endow cells with the ability to communicate with the external environment and make appropriate responses, which is crucial for cell survival and behavioral regulation [1,2]. Among them, signal transduction receptors play an important role, as they can respond to extracellular signals and transmit them to the interior of cells, triggering intracellular chemical processes and achieving signal transduction [3-5]. The two well-known important transduction receptors are receptor tyrosine kinases (RTKs) and G protein coupled receptors (GPCRs). RTKs achieve transmembrane signal transduction by triggering dimerization of transmembrane receptors, while GPCRs work by triggering global conformational changes in transmembrane protein structures. Although constructing artificial receptors that simulate these complex processes is highly challenging, it has shown great potential in the fields of life sciences and biomedical applications [6-8].

Up to now, a series of bionic or abiotic systems, in response to different stimulus like pH [9], ligand [10,11], redox [12,13], etc., have been developed to achieve artificial transmembrane signaling. Based on the work mechanism of RTKs, several unsymmetri-

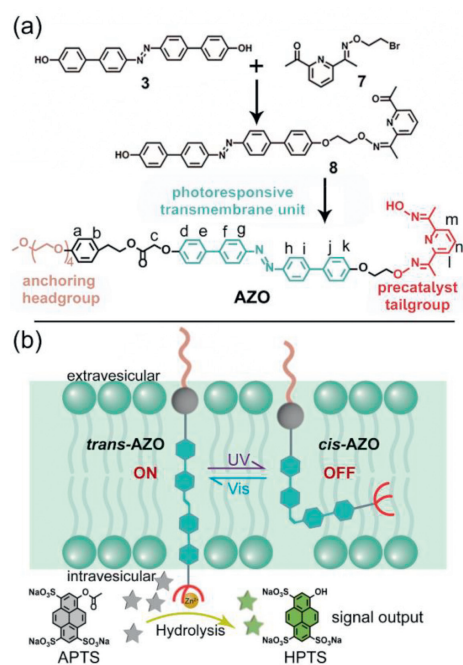
cal transmembrane receptors have been developed, which can respond to extravesicular signals to form dimerization and induce the switch-on of the intravesicular reactions [14-17]. Similarly, scientists also try to synthesize artificial receptors that have similar function as GPCRs, although it is widely believed that this is not easy. The most representative and well-known receptors are the helical α -aminoisobutyric acid oligopeptides that can alter their transmembrane structure in response to specific chemical [11] or physical stimuli [18]. Recently, we reported an artificial receptor that mimics GPCRs signal transduction by controlling conformational changes between the folding and unfolding of a transmembrane unit [19]. In addition to the simulating of RTKs and GPCRs, Hunter *et al.* created an alternative translocation mechanism to transmit a chemical signal across lipid membranes [9,13,20,21]. This abiotic mechanism was subsequently developed by the Liu's [22,23] and our group [24]. Despite continuous efforts are done to develop artificial transducers with new structures and mechanisms [25-27], the research field is still in its infancy.

Photoisomerization enable photo-responsive reversible changes in molecular conformation, which represents an important tool to achieve molecular motion in various environments [28-33]. This specific character led us to recognize that the photo-triggered molecular motion can serve as a new mechanism for signal transduction across a lipid membrane. Here, we present an azobenzene-

* Corresponding author.

E-mail address: baochunyan@ecust.edu.cn (C. Bao).

¹ These authors contributed equally to this work.



Scheme 1. (a) Molecular synthesis and structure of the designed receptor **AZO**. (b) Schematic representation of photoreversible "ON/OFF" switch of signal transduction.

based artificial receptor (**AZO**) to achieve transmembrane signaling (Scheme 1a), which contains three essential structural elements: an oligo(ethylene glycol) (OEG) headgroup, a photoresponsive biphenyl-azobenzene moiety and a pyridine-oxime tailgroup. The hydrophilic OEG is introduced to regulate the molecular polarity, so that **AZO** has an amphiphilic structure to match the lipid structures. And it also acts as the anchoring group to control the location of molecules in lipids. The rigid biphenyl-azobenzene moiety is used as the transmembrane unit, which can undergo significant molecular conformational changes through reversible isomerization upon light irradiation, thereby affecting the transmembrane molecular length. And the pyridine-oxime moiety is used as the pre-catalyst to catalyze 8-acetoxyppyrene-1,3,6-trisulfonate trisodium salt (APTS) ester hydrolysis when bound to Zn²⁺. As illustrated in Scheme 1b, before ultraviolet (UV) light irradiation, the entire molecule is expected long enough to across the hydrophobic lipid bilayer, so that the pyridine-oxime pre-catalyst can achieve the interior of vesicles and complex with Zn²⁺ to catalyze the hydrolysis reaction of APTS in the vesicles, thus producing a detectable fluorescence output signal (ON). Once UV irradiation is applied, the isomerization of azobenzene (from *trans*- to *cis*-isomer) would induce change of molecular conformation and reduce of molecular length, thus preventing the pre-catalyst tailgroup from complexing with the interior Zn²⁺ and stopping signal transduction (OFF). Finally, alternative UV and visible light irradiation would realize reversible signal transduction switching between "ON" and "OFF" states in a controlled manner.

To verify the rationalization of molecular design of **AZO**, the optimized molecular structures of both *trans*-**AZO** and *cis*-**AZO** were calculated according to the Corey-Pauling-Koltun (CPK) model. As shown in Fig. 1a, it showed molecular lengths of the hydrophobic parts were 3.2 nm (*trans*-**AZO**) and 2.0 nm (*cis*-**AZO**), respectively. Based on the hydrophobic core thickness of a typical phospholipid bilayer (~2.5 nm), the molecular lengths of *trans*-**AZO** and *cis*-**AZO** meet the requirements of molecular design. The detailed molecule state in the lipids was further studied by molecular dynamics (MD) simulations. Fig. 1b showed the snapshots of the systems before and after photoisomerization by using VMD software

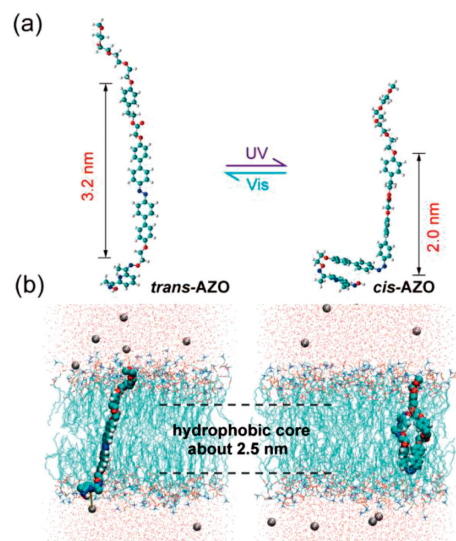


Fig. 1. (a) The optimized structures of *trans*-**AZO** and *cis*-**AZO**. (b) Their representative cross-section snapshots from a 20 ns equilibrium MD trajectory in a lipid bilayer.

[34]. As expected, *trans*-**AZO** is long enough to across the lipid bilayers in which the pre-catalyst tailgroup arrives the interior water phase to coordinate with Zn²⁺. After photoisomerization, the reduced molecular length pulls the pre-catalyst tailgroup into the lipids, so as to prevent the complexation with Zn²⁺. Further, the radial distribution function (rdf) between the N atom of the pre-catalyst group and Zn²⁺ were calculated. The *trans*-isomer exhibits a clear peak appeared at 1.5 nm, while the *cis*-isomer does not, indicating a distinct coordination between *trans*-**AZO** and Zn²⁺ (Fig. S1 in Supporting information). To further illustrate the role of OEG, a molecule **AZO1** without OEG substituent was designed for MD simulations (Fig. S2 in Supporting information). As expected, without the anchoring action of OEG, the pre-catalyst group of *cis*-**AZO1** can arrive the interior water phase, thus the catalytic hydrolysis would not be stopped.

AZO was synthesized and verified by ¹H, ¹³C nuclear magnetic resonance spectrum (NMR) and high resolution mass spectrum (HR-MS) (Figs. S9–S35 in Supporting information). The photoisomerization behavior of **AZO** was investigated by ultraviolet-visible (UV-vis) spectrum, where chloroform was used as the solvent due to the similar hydrophobic property to the phospholipid bilayer. As shown in Fig. 2a, **AZO** exhibited an intense π - π^* band around 380 nm and a weaker n - π^* band around 470 nm, showing typical *trans*-isomer characteristic. Upon UV irradiation, the peak around 380 nm decreased while the peak around 470 nm increased with an isosbestic point around 330 nm, exhibiting the generation of photoisomerization from *trans*- to *cis*-isomer (Fig. S3a in Supporting information) [35]. Subsequent irradiation with visible light led to reverse spectral changes (Fig. S3b in Supporting information), promoting the transition from *cis*- to *trans*-isomer. Apart from the initial inherent loss, **AZO** underwent reversible photoisomerization without detectable fatigue after multiple cycles (Fig. 2b). The successful photoisomerization was further confirmed by ¹H NMR spectroscopy (Fig. 2c). In addition, *cis*-isomer was relatively stable with a half-life ($t_{1/2}$) of 68 min in the dark by recording the change of UV-vis absorption (Fig. S4 in Supporting information). Relatively good stability provides a basis for the subsequent light-modulated signal transduction strategy.

An artificial liposome system based on large unilamellar vesicles (LUVs) was used to investigate transmembrane signal transduction of **AZO**. LUVs were prepared using egg yolk phosphatidyl-

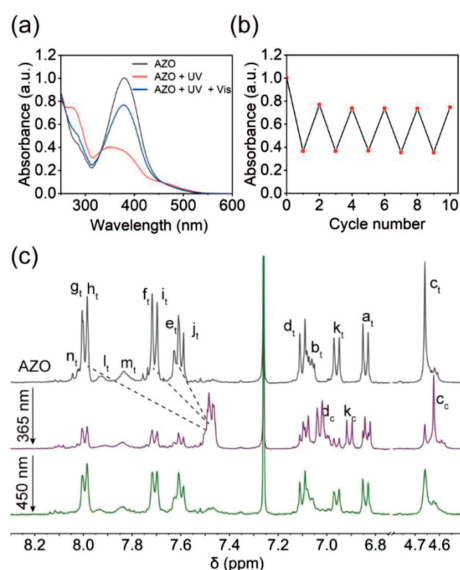


Fig. 2. (a) UV-vis spectrum of **AZO** in CHCl_3 (5.0×10^{-5} mol/L) and the corresponding spectra upon 365 and 450 nm irradiation. (b) Absorption changes at 380 nm after successive cycles of 365/450 nm irradiation. The irradiation condition is 0.5 min with intensity of 5 mW/cm^2 . (c) Partial ^1H NMR spectra (400 MHz, 298 K) of **AZO** (1×10^{-2} mol/L in CDCl_3) before (top) and after 365 nm irradiation (5 min, 10 mW/cm^2) (middle) and 450 nm irradiation (5 min, 10 mW/cm^2) (bottom). See Scheme 1a for proton assignments. Subscript “t” and “c” indicate the peaks assigned to *trans*- and *cis*-isomers, respectively.

choline (EYPC) while **AZO** was loaded in vesicular membrane at 2 mol% relative to lipid (LUVs \rightarrow AZO). Zinc chloride (0.5 mmol/L), APTS (0.5 mmol/L) and HEPES (100 mmol/L) buffer (pH 7.0) were encapsulated into the LUVs with a final lipid concentration of 1.0 mmol/L. A blank LUVs without **AZO** was prepared in the same manner. As an artificial receptor for signal transduction, another prerequisite is that the presence of **AZO** and its transduction process will not damage the lipid membrane. Therefore, dynamic light scattering (DLS) analysis was performed on the LUVs (Fig. 3a), which showed an average diameter of ~ 100 nm for LUVs \rightarrow AZO. Unlike the surfactant Triton X-100, subsequent UV and visible light irradiation had little effect on the integrity of LUVs (LUVs \rightarrow AZO+UV and LUVs \rightarrow AZO+UV+Vis), which can be further confirmed by the unchanged size and morphology in TEM images (Fig. S5 in Supporting information). Then, LUVs-based signal transduction assay was investigated, in which the time-dependent fluorescence intensity of 8-hydroxypyrene-1,3,6-trisulfonic acid (HPTS) generated by hydrolysis of APTS at 510 nm was tracked over a period of 24 h (Fig. 3b). It should be noted that only transducer molecules inserted with a correct orientation will produce a fluorescence signal, as supposed in Scheme 1b. As shown in Fig. 3b, compared with the blank system (LUVs), the fluorescence intensity of LUVs \rightarrow AZO significantly increased, indicating continuous hydrolysis of APTS in an “ON” state.

In order to ensure that the increased fluorescence is caused by APTS hydrolysis inside the vesicles rather than the leakage of LUVs, a fluorescence quenching experiment was performed on LUVs \rightarrow AZO by adding a membrane-impermeable hydrophilic fluorescent quencher *p*-xylene-bis-pyridinium bromide (DPX) (Fig. S6 in Supporting information). The insignificant change in the excitation spectra after 24 h confirmed that the hydrolyzed HPTS was encapsulated in the vesicles, indicating that **AZO** initiated APTS hydrolysis by extending the precatalyst tailgroup into the interior of the vesicles and complexing with Zn^{2+} . Taking into account the relative long half-life of the *cis*-isomer, LUVs-based signal transduction assay was also performed on *cis*-**AZO** (LUVs \rightarrow AZO+UV). The

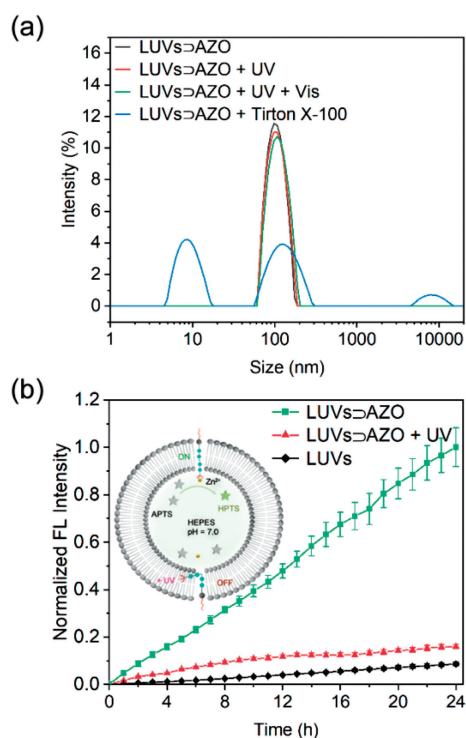


Fig. 3. (a) DLS analysis of LUVs containing **AZO** (LUVs \rightarrow AZO), subsequent UV (LUVs \rightarrow AZO+UV) and visible light irradiation (LUVs \rightarrow AZO+UV+Vis). (b) Evolution of time-dependent fluorescence intensity of LUVs, LUVs \rightarrow AZO and LUVs \rightarrow AZO+UV at 510 nm (exciting at 405 nm). An intermittent UV irradiation (LED 365 nm, 10 mW/cm^2) was used for LUVs \rightarrow AZO+UV. Inset is the schematic representation of the LUVs assay for detecting signal transduction activity. Data are presented as mean \pm standard error (SEM) ($n = 3$).

alternative change of absorption verified the successful isomerization of **AZO** in lipid membranes (Fig. S7 in Supporting information). An intermittent UV illumination mode of 20 s every 30 min was applied to ensure the *cis*-state of **AZO** in the lipids during the experiments (Fig. 3a). As expected, there was no significant fluorescent increase, showing an “OFF” state of signal transduction as supposed in Scheme 1b (Fig. 3b). In addition, the effect of Zn^{2+} on signal transduction was also investigated (Fig. S8 in Supporting information), and the results showed that it was indispensable and its concentration directly affected the hydrolysis rate of APTS. All these results illustrate that the isomers of **AZO** showed distinct “ON” and “OFF” states that trigger APTS hydrolysis within the vesicles.

Natural transmembrane signaling receptors can respond to extracellular signaling stimuli and reversibly switch signal transduction between the active and inactive states. Based on the reversible conformational conversion between *trans*-**AZO** and *cis*-**AZO**, light signal transduction of **AZO** was explored upon *in situ* UV and visible irradiation, as illustrated in Fig. 4. Initially, the precatalyst tailgroup of *trans*-**AZO** is activated by binding to zinc ions in the interior of the vesicles, which induces ester hydrolysis and fluorescence increase (from APTS to HPTS). The transmembrane receptor is in the “ON” state for signaling. After 2 h, UV light irradiation is applied to change the molecular conformation of **AZO** into *cis*-**AZO** in lipids by an intermittent UV irradiation. The reduced molecular length and the anchoring role of the OEG headgroup cause the precatalyst tailgroup to be pulled into the lipid membrane, thus preventing Zn^{2+} binding, stopping the catalytic action (no significant increase in fluorescence) and turning the signaling process in the “OFF” state. Then, visible light irradiation enables *cis*-**AZO** to recover back to *trans*-**AZO** and switches on signal transduction

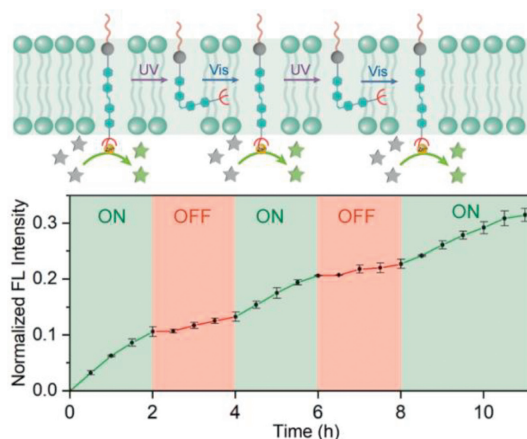


Fig. 4. Reversible “ON” and “OFF” switches of light signal transduction by alternating irradiation with UV and visible light. The upper figure is a schematic representation, and the lower figure shows the corresponding time-dependent fluorescence change at 510 nm (exciting at 405 nm). Data are presented as mean \pm SEM ($n=3$).

again (obvious increase in fluorescence). Finally, reversible “ON” and “OFF” switching of signal transduction (stepped increase in fluorescence) can be achieved by alternating UV and visible light irradiation.

In conclusion, we have demonstrated a novel artificial signal transduction receptor **AZO** that achieves light signal transduction through reversible conversion of molecular transmembrane conformations by photoisomerization. Reasonable and precise molecular design enables the synthesized receptor to achieve the expected goals. The significant change of molecular conformation and length between *trans*-AZO and *cis*-AZO results in activation or deactivation of the precatalyst moiety of **AZO** by controlling binding events in the vesicles, thus leading to reversible “ON” and “OFF” control of transduction process. We believe that our design offers more alternative solutions for developing of artificial receptors for signal transduction. And the light controllable intravesicular catalytic process has the potential applications in drug release, biomimetic catalysis and biosensing.

Declaration of competing interest

The authors declare that they have no known competing financial interests or personal relationships that could have appeared to influence the work reported in this paper.

CRediT authorship contribution statement

Kai Ye: Writing – original draft, Methodology, Investigation, Data curation, Conceptualization. **Zhicheng Ye:** Methodology, Data curation. **Chuantao Wang:** Methodology, Investigation. **Zhilai Luo:** Software, Formal analysis. **Cheng Lian:** Software, Data curation.

Chunyan Bao: Writing – review & editing, Validation, Supervision, Funding acquisition, Conceptualization.

Acknowledgments

This work was supported by the National Natural Science Foundation of China (No. 22171085) and Shanghai Frontier Science Research Base of Optogenetic Techniques for Cell Metabolism (Shanghai Municipal Education Commission, No. 2021 Sci & Tech 03–28). We thank the Research Centre of Analysis and Test of East China University of Science and Technology for the help with the characterization.

Supplementary materials

Supplementary material associated with this article can be found, in the online version, at doi:10.1016/j.ccl.2024.110033.

References

- [1] J. Pouyssegur, K. Seuwen, *Annu. Rev. Physiol.* 54 (1992) 195–210.
- [2] K.L. Pierce, R.T. Premont, R.J. Lefkowitz, *Nat. Rev. Mol. Cell Biol.* 3 (2002) 639–650.
- [3] S. Gavi, E. Shumay, H. Wang, C.C. Malbon, *Trends Endocrinol. Metab.* 17 (2006) 48–54.
- [4] M.A. Lemmon, J. Schlessinger, *Cell* 141 (2010) 1117–1134.
- [5] C. Kiel, E. Yus, L. Serrano, *Cell* 140 (2010) 33–47.
- [6] K. Shi, C. Song, Y. Wang, R. Chandrawati, Y. Lin, *Commun. Mater.* 4 (2023) 65.
- [7] Z. Quinn, W. Mao, Y. Xia, R. John, Y. Wan, *Bioact. Mater.* 6 (2021) 749–756.
- [8] H. Wu, L. Zheng, N. Li, et al., *J. Am. Chem. Soc.* 145 (2023) 2315–2321.
- [9] M.J. Langton, F. Keymeulen, M. Ciaccia, N.H. Williams, C.A. Hunter, *Nat. Chem.* 9 (2017) 426–430.
- [10] K. Bernitzki, M. Maue, T. Schrader, *Chem. Eur. J.* 18 (2012) 13412–13417.
- [11] F.G.A. Lister, B.A.F. Le Bailly, S.J. Webb, J. Clayden, *Nat. Chem.* 9 (2017) 420–425.
- [12] S. Liu, Y. Xing, T. Yan, et al., *Nano Res.* 16 (2023) 964–969.
- [13] L. Trevisan, I. Kocsis, C.A. Hunter, *Chem. Commun.* 57 (2021) 2196–2198.
- [14] P. Barton, C.A. Hunter, T.J. Potter, S.J. Webb, N.H. Williams, *Angew. Chem. Int. Ed.* 41 (2002) 3878–3881.
- [15] K. Bernitzki, T. Schrader, *Angew. Chem. Int. Ed.* 48 (2009) 8001–8005.
- [16] H. Chen, L. Zhou, C. Li, et al., *Chem. Sci.* 12 (2021) 8224–8230.
- [17] H. Chen, W. Xu, H. Shi, et al., *Angew. Chem. Int. Ed.* 62 (2023) e202301559.
- [18] M. De Poli, W. Zawodny, O. Quinero, et al., *Science* 352 (2016) 575–580.
- [19] S. Pang, J. Liu, T. Li, et al., *J. Am. Chem. Soc.* 145 (2023) 20761–20766.
- [20] M.J. Langton, N.H. Williams, C.A. Hunter, *J. Am. Chem. Soc.* 139 (2017) 6461–6466.
- [21] M.J. Langton, L.M. Scriven, N.H. Williams, C.A. Hunter, *J. Am. Chem. Soc.* 139 (2017) 15768–15773.
- [22] J. Hou, X. Jiang, F. Yang, et al., *Chem. Commun.* 58 (2022) 5725–5728.
- [23] J. Hou, J. Guo, T. Yan, et al., *Chem. Sci.* 14 (2023) 6039–6044.
- [24] H. Yang, S. Du, Z. Ye, et al., *Chem. Sci.* 13 (2022) 2487–2494.
- [25] H. Li, Y. Yan, J. Chen, et al., *Sci. Adv.* 9 (2023) eade5853.
- [26] A.B. Søgaard, A.B. Pedersen, K.B. Løvschall, et al., *Nat. Commun.* 14 (2023) 1646.
- [27] S.A. Gartland, T.G. Johnson, E. Walkley, M.J. Langton, *Angew. Chem. Int. Ed.* 62 (2023) e202309080.
- [28] E. Merino, M. Ribagorda, *Beilstein J. Org. Chem.* 8 (2012) 1071–1090.
- [29] Z.L. Pianowski, *Chem. Eur. J.* 25 (2019) 5128–5144.
- [30] J. Volarić, W. Szymanski, N.A. Simeth, B.L. Feringa, *Chem. Soc. Rev.* 50 (2021) 12377–12449.
- [31] Y. Zhu, P. Li, C. Liu, et al., *Chin. Chem. Lett.* 34 (2023) 107543.
- [32] C. Xiao, W.Y. Zhao, D.Y. Zhou, et al., *Chin. Chem. Lett.* 26 (2015) 817–824.
- [33] G. Liu, Y. Li, C. Tian, et al., *Chin. Chem. Lett.* 35 (2024) 109403.
- [34] W. Humphrey, A. Dalke, K. Schulten, *J. Mol. Graph.* 14 (1996) 33–38.
- [35] J. Zhu, X. Chen, X. Jin, Q. Wang, *Chin. Chem. Lett.* 34 (2023) 108002.